Finite element study the seismic behavior of connection to replace the continuity plates in (NFT/CFT) steel columns

Omid Rezaifar [**1] and Adel Younesi [*2]

[1] *Department of Civil Engineering and Research Institute of Novin Technologies, Semnan University, Iran*
[2] *Structure Engineering, Faculty of Civil Engineering, Semnan University, Iran*

Abstract. The use of box columns has been increased due to the rigidity in rigid orthogonal moment resisting frames. On the other hand, the installation and welding of necessary horizontal continuity plates inside the columns are both labor-consuming and costly tasks. Accordingly, in this paper, a new beam-to-box column connection by trapezoidal external stiffeners and horizontal bar mats is presented to provide seismic parameters. The proposed connection consists of eight external stiffeners in the level of beam flanges and five horizontal bar mats in Concrete Filled Tube (CFT) columns. The new connection effectively alleviates the stress concentration and moves the plastic hinge away from the column face by horizontal external stiffeners. In addition, the result shows that proposed connection has provided the required strength and rigidity of connection, so that the increased strength, 8.08% and rigidity, 3.01% are compared to connection with internal continuity plates, also the results indicate that this connection can offer appropriate ductility and energy dissipation capacity for its potential application in moment resisting frames in seismic region. As a result, the proposed connection can be a good alternative for connection with continuity plates.

Keywords: (NFT/CFT) column; rigid connection; continuity plate; trapezoidal stiffener; bar mats

1. Introduction

Steel tube columns with or without concrete filled are widely used in steel buildings due to their good seismic performance. To provide rigidity in these connections, continuity plates are commonly used in panel zone (PZ), but the installation and welding of necessary horizontal continuity plates inside the columns are both labour-consuming and costly tasks. Accordingly, the use of external stiffeners is enormous attention by researchers.

From 1930 onwards, numerous studies have been conducted on rigid connections of I-shaped beam to H- shaped column, but considerable studies haven't been done on the box columns. One of the most valid and inclusive researches has been done by (Lee *et al*. 1991a, b, 1993a, b, c and 1994). In their study, angle external stiffeners, triangular plates, T-shape and also continuity plate have been studied. The purpose of their paper is to find a proper external stiffener as an alternative for inner continuity plate to satisfy major factors of effective rigid connection. Accordingly, side

---

∗Corresponding author, M.Sc. Graduate, E-mail: a.younesi@students.semnan.ac.ir
∗∗ Assistant Professor, E-mail: Orezayfar@semnan.ac.ir

and intermediate connections have been studied. Research team concluded that connection with T-shaped stiffener has the best performance among other connections and is considered a good substitute for connection with inner continuity plate.

Wide experimental and analytical studies have been carried out since the 1970 onwards, mainly by (Krawinkler *et al.* 1971, Bertero *et al.* 1973, Popov 1987), in order to examine the behavior of PZ under monotonic and cyclic loadings.

Three types of traditional connections to rectangular CFT columns have been widely used in Asian countries such as China, Japan, and South Korea. Each employs an internal diaphragm, an external diaphragm, or a through diaphragm. These connections offer practical and economical advantages and their performance have been extensively studied. Previous investigations on the experimental behavior of these traditional connections have included that of (Azuma *et al.* 2000, Miura and Makino 2001, Mirghaderi *et al.* 2010, Shahabeddin *et al.* 2012, Iwashita *et al.* 2003, Nishiyama *et al.* 2004, Nie *et al.* 2008a, b, 2009, Jiang *et al.* 2009, Rong *et al.* 2012, and Qin *et al.* 2014a, b). Analytical study on the performance has been conducted by (Kurobane 2002, Fukumoto and Morita 2005, Nie *et al.* 2008a, b, 2009, Jones and Wang 2010, Wang *et al.* 2009, Qin *et al.* 2014a, b). It has been demonstrated that the use of diaphragms in the column locally not only stiffens the connection, but also results in strain concentration and fracture of the beam flange at their weld access holes. Meanwhile, discontinuities of welds arise from both the presence of weld access holes and difficulties in executing the welds, especially when sitting on the top flange of a deep beam. Furthermore, strain concentrations develop at connection details that lack a gradual transition in geometry and lead to a reduction in connection ductility.

(Kang *et al.* 2015) in their paper compared the previously proposed equations for joint shear capacity, discusses the shear deformation mechanism of the joint, and suggests recommendations for obtaining more accurate predictions. Finite element analyses of internal diaphragm connections to CFT columns were carried out in ABAQUS. Results show that: (1) shear deformation of the steel tube dominates the deformation of the joint; while the thickness of the diaphragms has a negligible effect; (2) in OpenSEES simulation, the joint behavior is highly dependent on the yielding strength given to the rotational spring; and (3) axial force ratio has a significant effect on the joint deformation of the specimen analyzed. Finally, modified joint shear force-deformation relations are proposed based on previous theory.

According to a study by (Qiu *et al.* 2013) Shear failure and core concrete crushing at plastic hinge region are the two main failure modes of bridge piers, which can make repair impossible and cause the collapse of bridge. To avoid the two types of failure of pier, a composite pier was proposed, which was formed by embedding high strength concrete filled steel tubular (CFT) column in reinforced concrete (RC) pier. Through cyclic loading tests, the seismic performances of the composite pier were studied. The experimental results show that the CFT column embedded in composite pier can increase the flexural strength, displacement ductility and energy dissipation capacity, and decrease the residual displacement after undergoing large deformation. (Wang and Chang 2013) in this paper presented a numerical study of axially loaded concrete-filled steel tubular columns with T-shaped cross section (CFTTS) based on the ABAQUS standard solver. Two types of columns with T-shaped cross section, the common concrete-filled steel tubular columns with T-shaped cross section (CCFTTS) and the double concrete-filled steel tubular columns with T-shaped cross section (DCFTTS), are discussed. The numerical results indicate that both have the similar failure mode that the steel tubes are only outward buckling on all columns' faces.

The major objective of the paper presented by (Kwak *et al.* 2013) is to evaluate the behavior

and ultimate resisting capacity of circular CFT columns. To consider the confinement effect, proper material models with respect to the confinement pressure are selected. (Huang *et al*. 2008) Proposed A method is proposed to estimate the ultimate strength of rectangular concrete-filled steel tubular (CFT) stub columns under axial compression.

In present study, the finite element software ANSYS is studied. In this paper, beam-to-Not Filled Tube (NFT) and CFT columns connections are resistant by various internal and external stiffeners in ten cases. Since the aim of the present study is to introduce a new connection and bolded it, it is compared with the analysis results.

2. Dimensions of the models

In this study, ten models with specifications are listed in the studied Table 1. In seven models, columns are filled with concrete but in other models, they are hollow. In all models, column is a square box, which is surrounded by I-beam of the four sides. (See Figs. 1 and 2).

Table 1 Models introduction (Sizes of models are in mm)

Names		NFT-0-00	CFT-0-00	NFT-I-00	CFT-I-00	CFT-0-B2	CFT-0-B4	CFT-0-B5	NFT-E-00	CFT-E-00	CFT-E-B5
Box column $H = 4000$	$B{\times}t$	450×25	450×25	450×25	450×25	450×25	450×25	450×25	450×25	450×25	450×25
I-Beam $L = 3000$	$b_f{\times}t_f$	200×15	200×15	200×15	200×15	200×15	200×15	200×15	200×15	200×15	200×15
	$h{\times}t_w$	400×8	400×8	400×8	400×8	400×8	400×8	400×8	400×8	400×8	400×8
	d	430	430	430	430	430	430	430	430	430	430
Hollow/ Filled		H	F	H	F	F	F	F	H	F	F
Bar mats		-	-	-	-	✓	✓	✓	-	-	✓
	d_b	-	-	-	-	25	25	25	-	-	25
Int. Stiffener		-	-	✓	✓	-	-	-	-	-	-
	t_s	-	-	15	15	-	-	-	-	-	-
	$a{\times}b$	-	-	400×400	400×400	-	-	-	-	-	-
	D	-	-	-	210	-	-	-	-	-	-
Ext. Stiffener		-	-	-	-	-	-	-	✓	✓	✓
	t_s	-	-	-	-	-	-	-	15	15	15
	b_s	-	-	-	-	-	-	-	212	212	212

Table 1 Continued

Names		NFT-0-00	CFT-0-00	NFT-I-00	CFT-I-00	CFT-0-B2	CFT-0-B4	CFT-0-B5	NFT-E-00	CFT-E-00	CFT-E-B5
Ext. Stiffener	b_{s1}	-	-	-	-	-	-	-	150	150	150
	l_s	-	-	-	-	-	-	-	500	500	500
	l_{s1}	-	-	-	-	-	-	-	515.4	515.4	515.4
	a_s	-	-	-	-	-	-	-	200	200	200
	a_{s1}	-	-	-	-	-	-	-	450	450	450

** CFT-E-B5 model is proposed connection

Fig. 1 Beam section

(a) NFT-0-00   (b) CFT-0-00   (c) NFT-I-00   (d) CFT-I-00   (e) CFT-0-B2

(f) CFT-0-B4   (g) CFT-0-B4   (h) NFT-E-00   (i) CFT-E-00   (j) CFT-E-B5(PC)
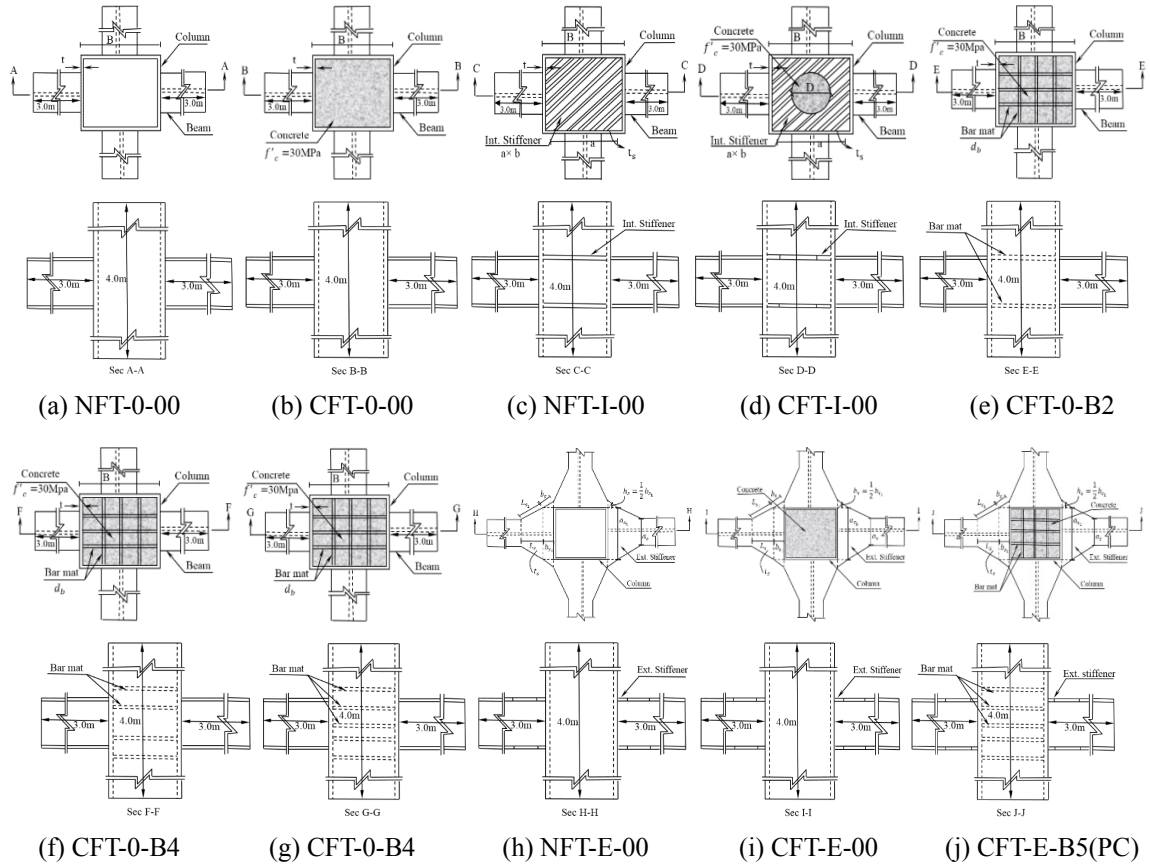
Fig. 2 Details of models

3. Finite Element Modeling (FEM)

In this paper, using the finite element software ANSYS for modeling of connections, since the type of materials, element, boundary condition and loading is effective, therefor in this section all of them are presented.

3.1 Material properties

According to Table 2, the materials used in mentioned models are steel and concrete. In this study, the Steel behavior is assumed elastic-perfect plastic (yield criterion is selected Von Mises). Since concrete is confined, this parameter has been observed in the behavior of concrete.

To model of steel structure, different elements including SOLID, SHELL can be used. The 4 nodes 3D shell element SHELL181 has been used in this study. The element considers the effects of bending and membrane deformation as well. The element has 6 Degree Of Freedom (DOF) in each node including three translational DOF of *Ux*, *UY* and *UZ* (are degrees of transportation freedom) along with three coordinate's axes and three rotational DOF of ROT. *X*, *Y* and *Z* (are degrees of rotation freedom) as well as three coordinate's axes. This element can model components with different thickness. Thickness is defined in element nodes and changes linearly between each two thickness nodes.

Table 2 Material properties

Materials	f_y (MPa)	f_u (Mpa)	$f\prime_c$ (MPa)	E (Mpa)	ϑ	Specific gravity $\left(\dfrac{kN}{m^2}\right)$
Steel	240	370	-	2×10^5	0.3	78.55
Concrete	-	-	30	0.27×10^5	0.2	24.00

3.2 Boundary conditions and loading

It is seen in Fig. 3, the models used in this study are as intermediate connection in which 4 beams at 3000 mm length have been connected to a box column at 4000 mm length. The end of each beams and column foot is located on 3D joint support. Boundary conditions are such a way that all translational DOFs have been bounded at one point on beams end and column foot.
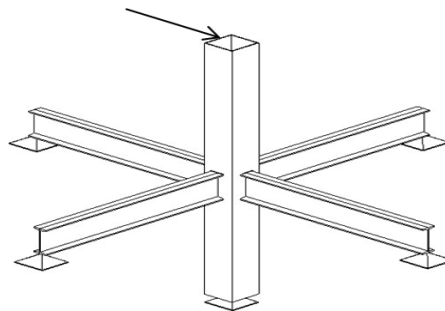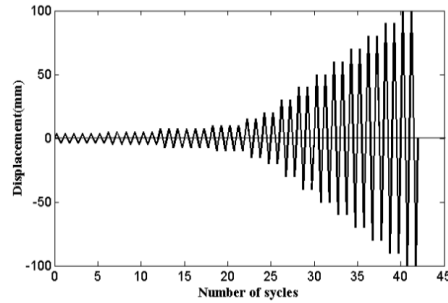

Fig. 3 Modeling setup

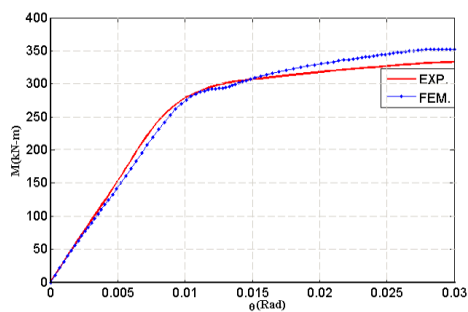Fig. 4 Time history diagram of loading, SAC97 (Clark 1997)

In this paper, two analyses have been done to study the accurate behavior of the connection, including monotonic static analysis and Hysteresis analysis. Diagram of time history for loading are illustrated in the Fig. 4, according to loading pattern SAC97 (Clark 1997).
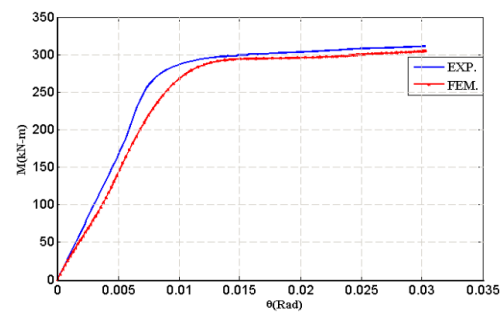
4. Experimental verification

The Finite Element Modeling (FEM) developed in this study is verified against the experimental data of connections stiffened with continuity plate (internal stiffener) and T-stiffener (external stiffener). The verification is performed for square columns stiffened with T-stiffener and continuity plate tested by (Lee *et al*. 1991a, b). In their paper, eight specimens, T-stiffener, angle and internal stiffener in various sizes are tested and results of two specimens (Table 3) are

Table 3 Details of test specimens (Lee *et al*. 1993a, b)

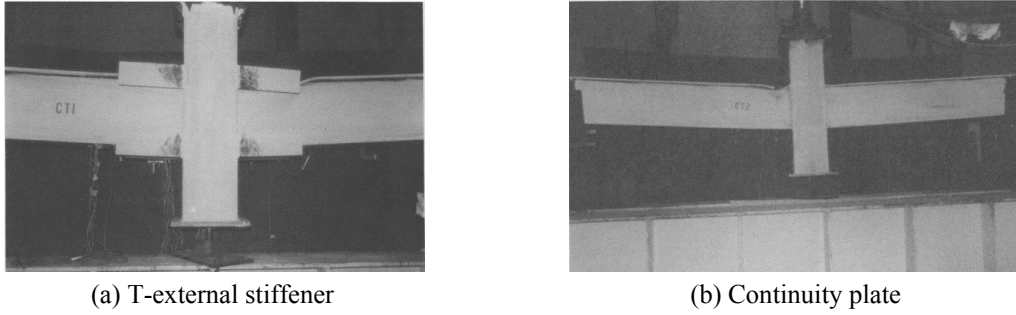| Specimen	Beam size mm×mm×(Kg/m)	Column size mm×mm×(Kg/m)	Stiffener type
MT1	$305 \times 165 \times 38.69$	$250 \times 250 \times 9$	T-Stiffener (300 mm long)
MT3	$305 \times 165 \times 38.69$	$250 \times 250 \times 9$	Internal stiffener (12 mm thick)

(a) T-external stiffener   (b) Continuity plate

Fig. 5 Compare the results of exp. (Lee *et al*. 1991a, b) model and FEM

<table>
<tr><td>(a) T-external stiffener</td><td>(b) Continuity plate</td></tr>
</table>

Fig. 6 Test set up (Lee *et al.* 1991a, b)

compared with FEM ones in the form of moment-rotation curves (Fig. 5). According to Fig. 5, comparing the results confirms the validity of the modeling with FEM.

5. Result and discussion

5.1 Ductility and rigidity

Strength, rigidity and ductility are important parameters in study of connection behavior. Ultimate strength is peak of force-displacement curve and ductility is the ability of a member or structure in deformations after yielding and rigidity are the property of a structure that it does not bend or flex under an applied force. Rigidity as follows the ability to load bearing by connections.

Ductility parameter of connections is defined by Eq. (1) and Fig. 7 and rigidity parameter is defined by Eq. (2) and Fig. 8.

$$\mu = \frac{\Delta_{max}}{\Delta_y} \tag{1}$$

Where μ is the ductility index, Δ_{max} and Δ_y are shown in Fig. 7.

$$R = \frac{K_i}{K_{total}} \times 100 \tag{2}$$
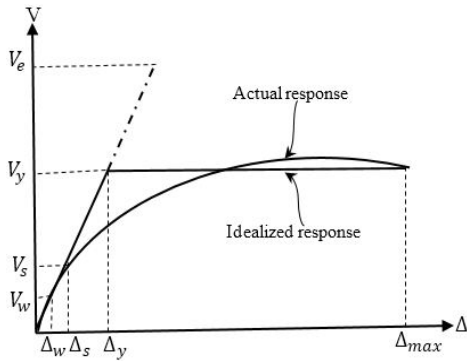

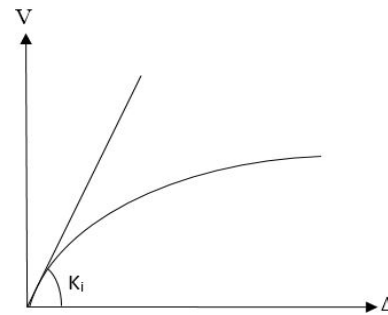Fig. 7 Actual and ideal response curves of connection

Fig. 8 Determination of stiffness

Where *R* is the rigidity, K_i is the stiffness and $K = \sum \dfrac{3EI}{L^3}$; EI is the flexural rigidity of each member of the connection and *L* is the length of each member.

5.2 In-filled concrete

Concrete in tube increased the flexural rigidity (EI) of column section under lateral load and increased the axial rigidity (EA) under compression load, therefore filled tube with concrete improved seismic parameters, result of FEM analysis shown in Table 4 and Fig. 9.

Notably, Eq. (3) is model without concrete.

$$\text{Hollow}: \quad (EI)_{tube} = E\left[2\frac{tB^3}{12} + 2(B-2t)t\left(\frac{B-t}{2}\right)^2 + 2\frac{Bt^3}{12} \right] \tag{3}$$

$$\text{Filled}: \quad \sum (E_iI_i) = (EI)_{tube} + (EI)_{core} = (EI)_{tube} + \frac{(B-2t)^4}{12} \tag{4}$$

There is an additional sentence, $\dfrac{(B-2t)^4}{12}$ in Eq. (4) indicates concrete increasing rigidity of connection and finally increases ultimate strength and stiffness. On the other hand, it increases the
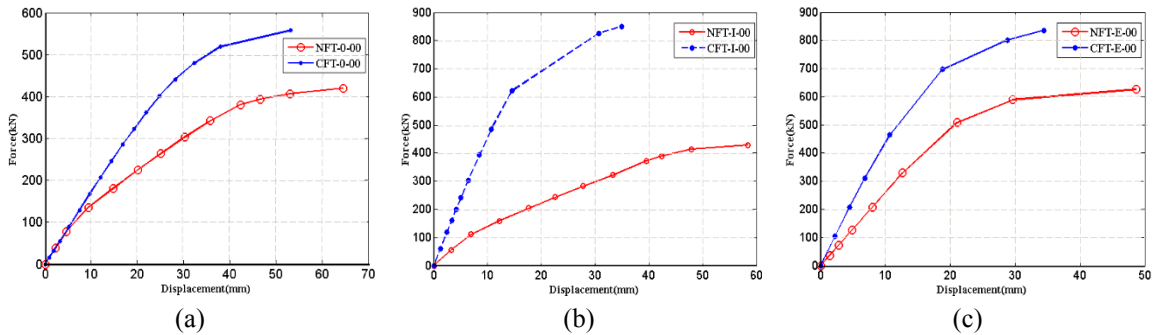

Fig. 9 Investigate of concrete effect on the Force-Displacement curves

Table 4 Concrete effect on seismic parameters

Models		Rigidity (*R*%)	Increment ratio (%)	Ductility μ	Increment ratio (%)	Strength P_{max} (kN)	Increment ratio (%)
Hollow/ Filled	NFT-0-00	76.39	+11.76	3.77	-2.92	41.93	+33.01
	CFT-0-00	85.37		3.66		55.77	
Int. Stiffener	NFT-I-00	93.37	+0.12	5.82	+4.98	42.84	+96.92
	CFT-I-00	93.48		6.11		84.36	
Ext. Stiffener	NFT-E-00	94.11	+1.74	5.57	-19.93	62.59	+35.95
	CFT-E-00	95.75		4.46		85.09	

effective surface in bearing. Finally, leading to a jump in the curves and the use of continuity plates and external stiffeners caused effect of these parameter increases.

According to Table 4, filling tube with concrete in NFT and NFT-E-00 models increases rigidity about 11.76%, 1.74% and strength increase 33.01%, 35.95 but ductility decreases about 2.92%, 19.93%. However, all related parameter increase in NFT-I-00 usage concrete increases all of these parameters. Filling column with concrete increases rigidity parameter (EI) and general stiffness of structure and finally, it increases strength and rigidity of connections.

5.3 Continuity plates and external stiffeners

A traditional method for rigid connection in box column is to use continuity plates in panel zone. The installation and welding of necessary horizontal continuity plates inside the columns are both labour-consuming and costly tasks. Accordingly, a new beam-to-box column connection by trapezoidal external stiffener is presented to provide seismic parameters. The presented connection consists of eight external stiffeners in the level of beam flanges. In another hand, this connection has a specific geometry; therefore, plastic hinge moved to beam.

5.3.1 Continuity plates

The use of continuity plates in panel zone of NFT-0-00 model does not have significant effect on the behavior of the connection, but in CFT-0-00 model, it increases seismic parameters, this topic is well-shown in Fig. 10(a).

According to Fig. 10(a)-(b), the reason of increased ultimate strength and the curve slop in elastic region (K_i) is continuity plate; considering the interaction sheet with concrete, the behavior of connection is improved noticeably.

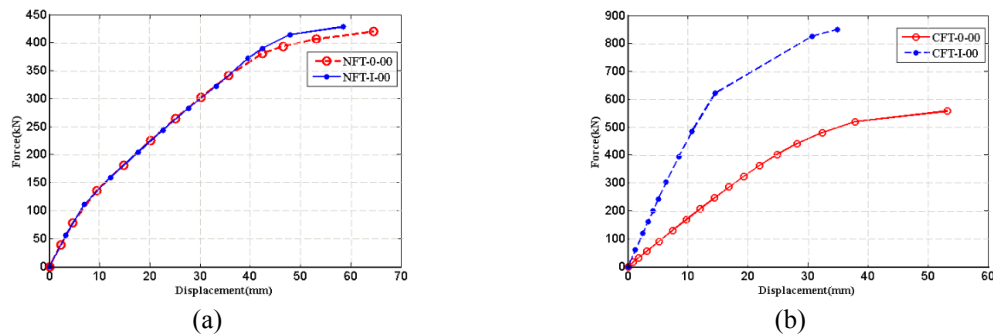(a)   (b)

Fig. 10 Investigate of existence of Int. stiffeners effect on the Force-Displacement curves

Table 5 Internal stiffeners effect on seismic parameters

	Models	Rigidity (R%)	Increment ratio (%)	Ductility μ	Increment ratio (%)	Strength P_{max} (kN)	Increment ratio (%)
Hollow	NFT-0-00	76.39	+22.22	3.77	+54.38	41.93	+2.17
	NFT-I-00	93.37		5.82		42.84	
Filled	CFT-0-00	85.37	+9.50	3.66	+66.94	55.77	+51.26
	CFT-I-00	93.48		6.11		84.36	

5.3.2 External stiffeners

Many studies have been done to find a specific geometry of the external stiffener. In addition, seismic parameters do load transfer duty well and confidently. In this study, a type of special connection is presented and then its adequacy is investigated.

According to Fig. 11, the use of external stiffener in hollow and filled column has shown almost similar effects and as well as increases strength and rigidity, that is the desired of AISC design code. The reason of this growth is special geometry and increase of stiffness around the panel zone and away the stress concentration from the column face. The effect of these stiffeners is presented in Table 6 qualitatively and quantitatively.
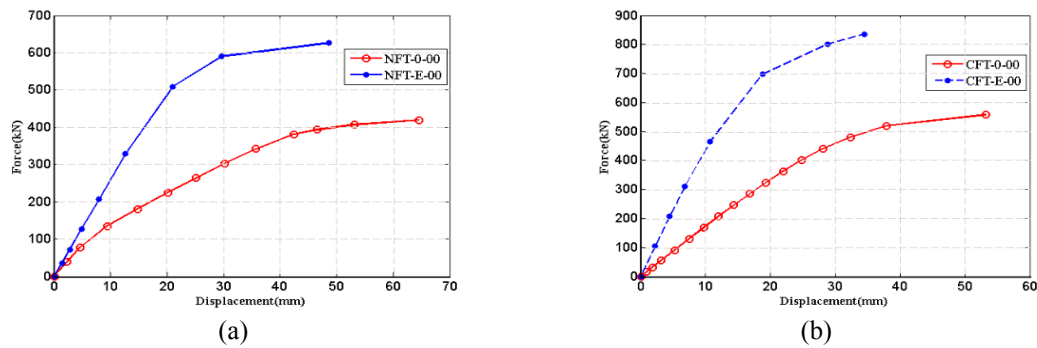

| (a) | (b) |

Fig. 11 Investigation of existence of Ext. stiffeners effect on the Force-Displacement curves

Table 6 External stiffeners effect on seismic parameters

Models		Rigidity (R%)	Increment ratio (%)	Ductility μ	Increment ratio (%)	Strength P_{max} (kN)	Increment ratio (%)
Hollow	NFT-0-00	76.39	+23.20	3.77	+47.75	41.93	+49.27
	NFT-E-00	94.11		5.57		62.59	
Filled	CFT-0-00	85.37	+12.16	3.66	+21.86	55.77	+52.57
	CFT-E-00	95.75		4.46		85.09	

5.3.3 The comparison between continuity plate and external stiffener

Since the continuity plates is removed and replaced by external stiffener in the proposed study, it can be a good understanding of proposed connection for providing seismic parameters and facilitating the performance. Therefore connection with continuity plates is compared to external stiffeners.

According to Figs. 12(a)-(b) and Table 7, external in hollow column (NFT) has behavior much better than continuity plate, the reason is muscular geometry and gradual increase of beam flange wide around the panel zone but in CFT column, since concrete is damaged prior to steel, so before connection achieves to high stiffness and additional strength the help of external stiffeners is failed. Accordingly, connections stiffed by continuity plate and external stiffeners have the similar behavior in CFT columns.

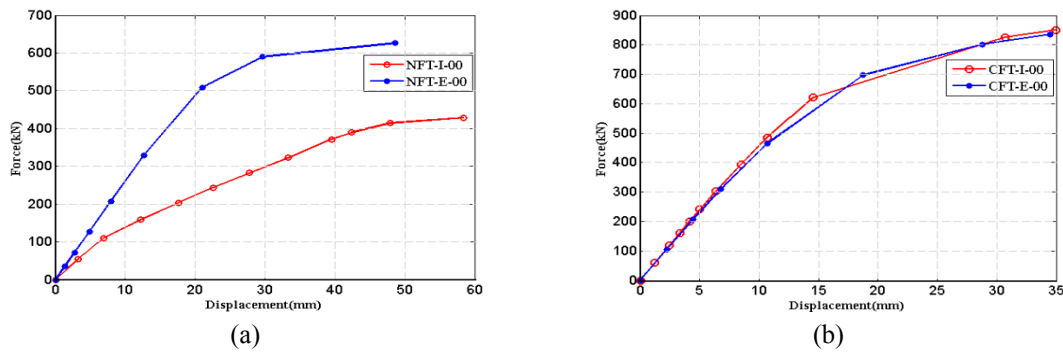(a)   (b)

Fig. 12 Investigation replacement Ext. stiffener instead of continuity plate

Table 7 Effect of replacement Ext. stiffener instead of Cont. plate on the seismic parameters

Models		Rigidity ($R\%$)	Increment ratio (%)	Ductility μ	Increment ratio (%)	Strength P_{max} (kN)	Increment ratio (%)
Hollow	NFT-I-00	93.37	+0.79	5.82	-4.30	42.84	+46.10
	NFT-E-00	94.11		5.57		62.59	
Filled	CFT-I-00	93.48	+2.43	6.11	-27.00	84.36	+0.86
	CFT-E-00	95.75		4.46		85.09	

5.4 Horizontal bars and comparison with continuity plate and external stiffeners

5.4.1 Effect of bar mats number

Since the use of continuity plate suggested AISC design code, therefore, horizontal bar mats was used in panel zone. In this section, the behavior of the connection is compared in three cases; two, four and five horizontal bar mats. Results are presented in Fig. 13 and Table 8.

As shown in Fig. 13(a), increasing the number of mats stiffness and strength must be from the models with lower mats. Fig. 13(b) shows that the use of five bar mats in CFT-E-00 model increases all of seismic parameters. Therefore, proposed model is a good connection in CFT columns for earthquake-prone areas.

(a)   (b)
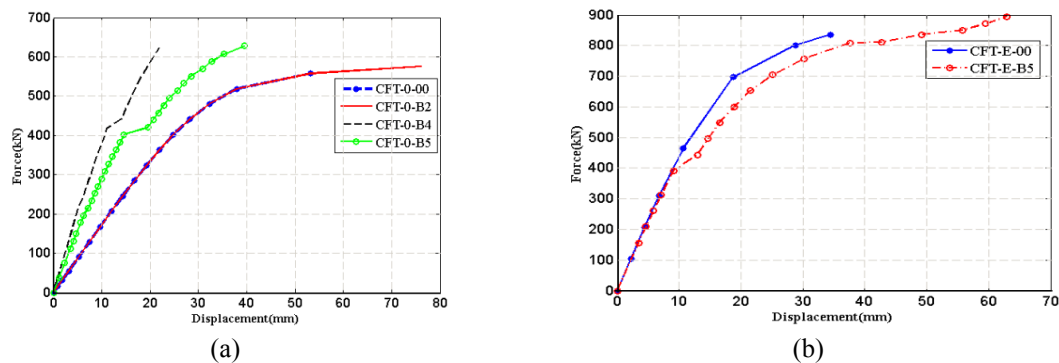
Fig. 13 Investigate of existence of horizontal bar mats effect on the Force-Displacement curves

Table 8 Horizontal bar mats effect on seismic parameters

Models		Rigidity (R%)	Increment ratio (%)	Ductility μ	Increment ratio (%)	Strength P_{max} (kN)	Increment ratio (%)
Bar mats	CFT-0-00	85.37		3.66		55.77	
	CFT-0-B2	92.01	+7.78	3.82	+4.37	57.73	+3.51
	CFT-0-B4	93.34	+9.34	4.01	+9.56	62.18	+11.49
	CFT-0-B5	94.28	+10.44	4.20	+14.75	62.76	+12.53
Ext. stiffener	CFT-E-00	95.75		4.46		85.09	
	CFT-E-B5	96.18	+0.45	7.04	+57.85	89.45	+5.12

Table 8 shows that the increased number of mats causes to increase all of parameters because it creates a good load transfer way. In CFT-E-00 model with assemble five bar mats in panel zone, strength and ductility parameters increases. In the other hand, CFT-E-00 and CFT-E-B5 connections move the plastic hinge away from the column face and provide as well Week beam-Strong column theory.

5.4.2 Comparison with continuity plate

The use of bar mats instead of continuity plates is not suitable, as shown in Fig. 14. The results in Table 9 include the absolute values and increment ratios for each of parameters. The use of bar mats in two, four and five numbers don't have positive effect against the continuity plate.

Since, area of mats is small and under load and cracking concrete, the bar mats are buckled and debonding not effective in bearing and load transfer.
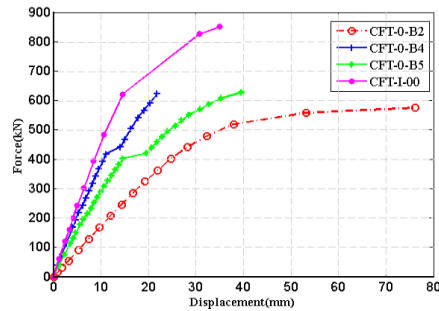

Fig. 14 Investigation of replacement bar mats instead of continuity plate

Table 9 Effect of replacement horizontal bar mats instead of Cont. plate on the seismic parameters

Models		Rigidity (R%)	Increment ratio (%)	Ductility μ	Increment ratio (%)	Strength P_{max} (kN)	Increment ratio (%)
Filled	CFT-I-00	93.48		6.11		84.36	
	CFT-0-B2	92.01	-1.57	3.82	-37.64	57.72	-31.58
	CFT-0-B4	93.34	-0.15	4.01	-34.37	62.18	-26.29
	CFT-0-B5	94.28	-0.86	4.20	-31.26	62.76	-25.60

5.4.3 Compare with external stiffener

In this section, connection with Ext. stiffener is compared to connection with two, four and five bar mats and their behavior is shown in Fig. 15. The slope of the linear region CFT-E-00 model is more than other models, therefore, stiffness and rigidity are more.

According to the results of analysis are presented in Table 10, model with external in CFT column is better than models with bar mats. Therefore, this connection suggested by authors.
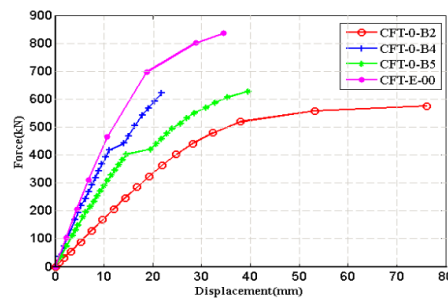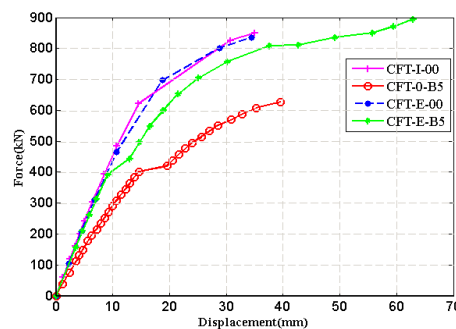

Fig. 15 Comparison the behavior of Ext. stiffener with bar mats

Table 10 Effect of replacement Ext. stiffener instead of horizontal bar mats on the seismic parameters

	Models	Rigidity ($R\%$)	Increment ratio (%)	Ductility μ	Increment ratio (%)	Strength P_{max} (kN)	Increment ratio (%)
Filled	CFT-E-00	95.75		4.46		85.09	
	CFT-0-B2	92.01	-3.91	3.82	-14.35	57.72	-32.17
	CFT-0-B4	93.34	-2.52	4.01	-10.09	62.18	-26.92
	CFT-0-B5	94.28	-1.54	4.20	-5.83	62.76	-26.24

5.5 Proposed connection (*CFT-E-B5*)

In this paper, a new connection with eight trapezoidal external stiffeners and five horizontal bar mats in CFT column are suggested. This model is the combination of CFT-E-00 and CFT-0-B5. The proposed connection plays the vital role of the continuity plate in panel zone and provides seismic parameters. On other hand, this connection reduced stress ratio around the connection and

ig. 16 Investigation the behavior of proposed connection

Table 11 Comparison of seismic parameters in proposed connection with another three models

	Models	Rigidity (R%)	Increment ratio (%)	Ductility μ	Increment ratio (%)	Strength P_{max} (kN)	Increment ratio (%)
Filled	CFT-E-B5	96.18		7.04		89.45	
	CFT-E-00	95.75	-0.45	4.46	-36.65	85.09	-4.87
	CFT-0-B5	94.28	-1.98	4.2	-38.92	62.76	-29.84
	CFT-I-00	93.48	-2.81	6.11	-13.21	84.36	-5.69

moved plastic hinge in beam. A comparison has been done between proposed connection and another three models (Fig. 16 and Table 11).

According to Fig. 16, around the load of 400 kN, models of CFT-I-00, CFT-E-00 and CFT-E-B5 have similar behavior but the behavior of CFT-0B5 model differs. Moreover, from 400 kN to 800kN, the behavior of these three models is almost similar due to existence of external stiffeners.

Table 11 shows that in models with external stiffener, strength and rigidity are more but ductility is less. If it is compared with the proposed model has best performance between all of models in this study. This connection has achieved the highest level of ductility. This connection is an effective model for NFT and CFT columns to provide seismic parameters and replace continuity plate.

5.6 Stiffness degradation

The stiffness degradation and its degradation rate in connection are very important. The number of connections has high initial stiffness but over time and increased load, it leads to deterioration that is not suitable. For investigation of this parameter in this section, stiffness degradation curves of all models are shown in Figs. 17(a) to (d).

As shown in Fig. 17(a), initial stiffness behaviours of both models are similar. NFT-0-00 model to displacement 10 mm has the most deterioration. But, after it reduced rate of stiffness deterioration. According to Fig. 17(b), initial stiffness of model with two bar mats is more than the two other models and rate of stiffness deterioration in the model with four bar mats is more than other models. Jump in curves is due to being bar mats in CFT column and makes a wobble. Initial
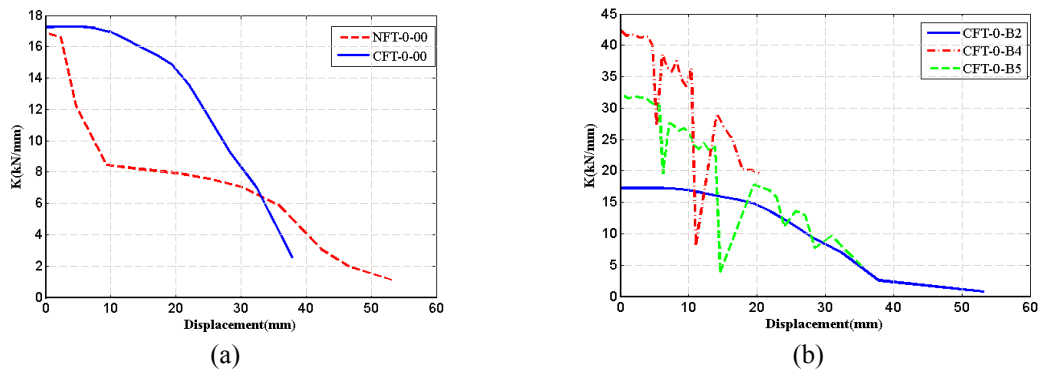

(a)   (b)

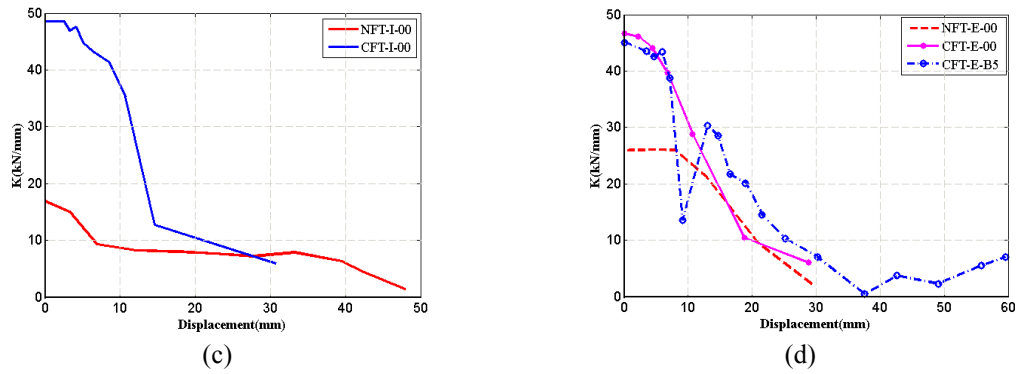Fig. 17 Stiffness deterioration curves

(c)

(d)

Fig. 17 Continued

stiffness of CFT-I-00 model is about three times that of NFT-I-00 model. In other hand, the reduced rate of stiffness is more than NFT-I-00 model too.

Fig. 17(d) shows the initial stiffness of CFT-E-00 and CFT-E-B5 models because bar mats and concrete are more than that of NFT-E-00 model. In addition, rate of stiffness deterioration of NFT-E-00 model is more than another models, that the reason is concrete existence column. In Fig. 17(d), jumping is seen similar to Fig. 17(b).

5.7 Stress distribution

Von Mises stress distribution of connections has been shown in Fig. 18. The use of trapezoidal external stiffeners causes proper and smooth distribution around panel zone and directs location of plastic hinge formation toward a safe and controlled area inside the beam and meets idea of weak beam- strong column approved by design codes.
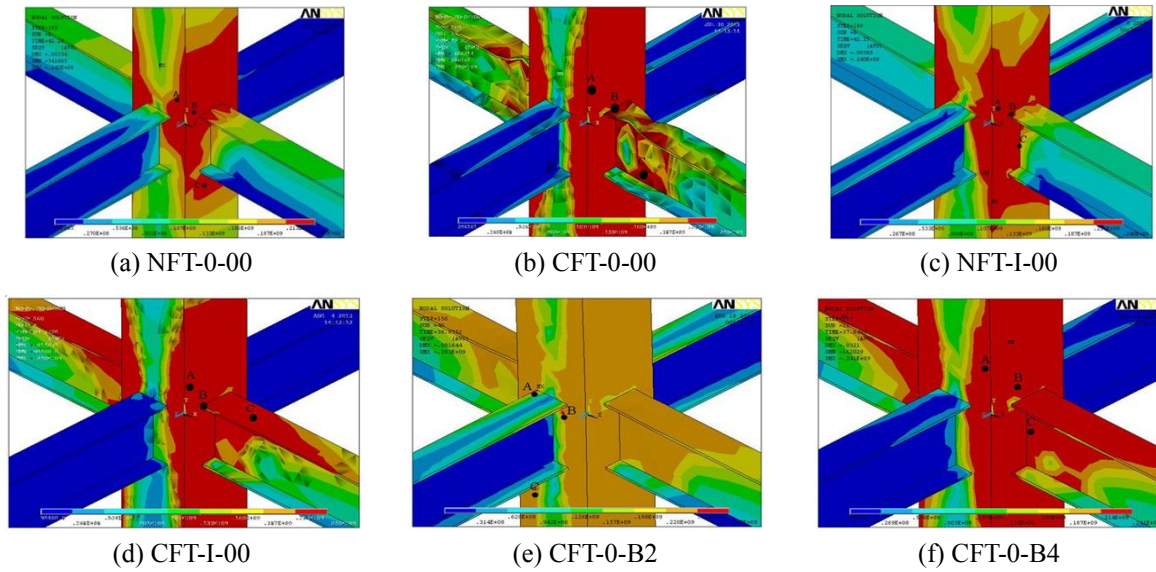

(a) NFT-0-00

(b) CFT-0-00

(c) NFT-I-00

(d) CFT-I-00

(e) CFT-0-B2

(f) CFT-0-B4

Fig. 18 Von Mises stress distribution

(g) CFT-0-B5

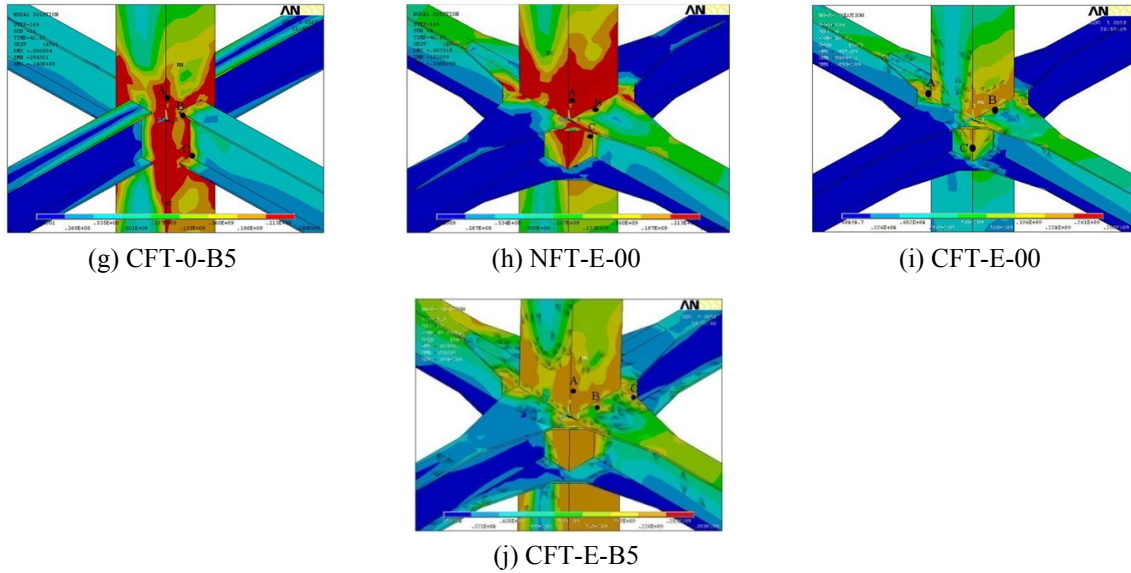(h) NFT-E-00

(i) CFT-E-00

(j) CFT-E-B5

Fig. 18 Continued

5.8 Hysteresis curves and energy dissipation

5.8.1 Hysteresis curves

Loops number of hysteresis curves and their envelope show the behavior of connection under cyclic load. The realization of the connection behavior under cyclic load should be extracted from hysteresis curves of connection. Accordingly, top of column is applied under cyclic load and has been extracted from curves behavior.

Figs. 19(a)-(b) show hysteresis curves of NFT-0-00 and CFT-0-00 models, moreover, CFT-0-00 model has less displacement and higher strength.

Fig. 19(c) shows the effect of concrete on the cyclic behavior of box column with internal stiffener. Concrete in CFT-I-00 model increases strength about 133% and decreases ultimate displacement.

According to Fig. 19(d), cyclic behavior is similar in models with two and four bar mats and puts together hysteresis curves of both model. But, in model with five bar mats, it increases strength and decreases ultimate displacement because adding the number of networks increases stiffness. The use of external stiffener is proposed in this study, and Fig. 19(e) shows these curves and the effect of concrete on the behavior of NFT-E-00 model. Existence of the concrete in box column has wider hysteresis curve.

According to Fig. 19(f), the proposed model has wider hysteresis curve among the all models. Strength of this model is 2000 kN. It is more than all of models. Therefore, CFT-E-B5 model is best one to replace it by continuity plate.

5.8.2 Energy dissipation

Energy dissipation is an important parameter for investigation of connection. Table 12 shows absolute and relative values of the energy dissipation. As for fixed of connection is used of continuity plate, therefor, results were compared with NFT-I-00 model.

Table 12 Energy dissipation of models

Models	$E_{(i)}(J)$	$\dfrac{E_{(i)}}{E_{(NFT-I-00)}} \times 100$
NFT-0-00	17597.00	69.69
CFT-0-00	13905.67	55.07
NFT-I-00	25249.19	100
CFT-I-00	19220.00	76.12
CFT-0-B2	14338.20	56.78
CFT-0-B4	15875.72	62.88
CFT-0-B5	16410.02	65.00
NFT-E-00	25859.69	118.26
CFT-E-00	19800.00	78.41
CFT-EB5	27619.14	109.39

6. Conclusions

In present study, ten connection were investigated. In these models, the effect of concrete, internal and external stiffeners and their interaction effects were studied. Within the scope of this paper, the following conclusions were drawn:

- In CFT models with internal stiffeners, the behavior of model with continuity plate is much better than models with bars mats, because it is completely jointed to the column flanges.
- External stiffeners increase parameters of rigidity, strength and ductility compared to connections with continuity plates and solved problem of defect implementation as well as uncertain continuity plates. On the other hand, it increases the width of the beam flange around the connection and provides as well week beam-strong column theory.
- The proposed connection has many load transfer directions therefore, it has achieved to best performance between all connections. On other hand, the effect of interaction concrete, bar mats and stiffeners in this connection specially establish behavior of this connection.

References

Azuma, K., Kurobane, Y. and Makino, Y. (2000), "Cyclic testing of beam-to-column connections with weld defects and Assessment of safety of numerically modeled connections from brittle fracture", *Eng. Struct.*, **22**(12), 1596-1608.

Bertero, V.V., Krawinkler, H. and Popov, E.P. (1973), "Further studies on seismic behavior of steel beam-column subassemblages", Report No. EERC-73/27; Earthquake Eng. Research Center, University of California, Berkeley, CA, USA.

Clark, P. (1997), "Protocol for fabrication, inspection, testing, and documentation of beam-column connection test and other experimental specimen", SAC Joint Venture, Sacramento, CA, USA.

Fukumoto, T. (2005), "Steel-beam-to-concrete-filled-steel-tube-column moment connections in Japan", *Steel Struct.*, **5**(4), 357-365.

Fukumoto, T. and Morita, K. (2005), "Elastoplastic behavior of panel zone in steel beam-to-concrete filled steel tube column moment connections", *J. Struct. Eng.*, **131**(12), 1841-1853.

Huang, Y.S., Long, Y.L. and Cai, J. (2008), "Ultimate strength of rectangular Concrete-Filled steel Tubular (CFT) stub columns under axial compression", *Steel Compos. Struct., Int. J.*, **8**(2), 115-128.

Iwashita, T., Kurobane, Y., Azuma, K. and Makino, Y. (2003), "Prediction of brittle fracture initiating at ends of CJP groove welded joints with defects: Study into applicability of failure assessment diagram approach", *Eng. Struct.*, **25**(14), 1815-1826.

Kwak, J.H., Kwak, H.G. and Kim, J.K. (2013), "Behavior of circular CFT columns subject to axial force and bending moment", *Steel Compos. Struct., Int. J.*, **14**(2), 173-190.

Jiang, X.L., Miao, J.K. and Chen, Z.H. (2009), "Experiment on seismic performance of diaphragm-through joint between concrete-filled square steel tubular column and steel beam", *J. Tianjin Univ.*, **42**(3), 194-200.

Jones, M.H. and Wang, Y.C. (2010), "Tying behavior of fin-plate connection to concrete-filled rectangular steel tubular column-development of a simplified calculation method", *J. Const. Steel Res.*, **66**(1), 1-10.

Kang, L., Leon, R.T. and Lu, X. (2015), "Shear strength analyses of internal diaphragm connections to CFT columns", *Steel Compos. Struct., Int. J.*, **18**(5), 1083-1101.

Krawinkler, H., Bertero, V.V. and Popov, E.P. (1971), "Inelastic behavior of steel beam-to-column subassemblages", Report No EERC-71/7; Earthquake Engineering Research Center, University of California, Berkeley, CA, USA.

Kurobane, Y. (2002), "Connections in tubular structures", *Prog. Struct. Eng. Mat.*, **4**(1), 35-45.

Lee, S.L., Ting, L.C. and Shanmugam, N.E. (1991a), "Behavior of I-beam to box-column connection stiffened externally and subjected to fluctuating loads", *J. Constr. Steel Res.*, **20**(2), 129-148.

Lee, S.L., Ting, L.C. and Shanmugam, N.E. (1991b), "Box column to I-beam connections with exter-nal stiffeners", *J. Constr. Steel Res.*, **18**(3), 209-226.

Lee, S.L., Ting, L.C. and Shanmugam, N.E. (1993a), "Design of I-beam to box-column connections stiffened externally", *Eng. J.*, **30**(4), 141-149.

Lee, S.L., Ting, L.C. and Shanmugam, N.E. (1993b), "Static behavior of I-beam to box-column connections with external stiffeners", *Eng. Struct.*, **71**(15), 269-275.

Lee, S.L., Ting, L.C. and Shanmugam, N.E. (1993c), "Use of external T-stiffeners in box-column to I-beam connections", *J, Constr. Steel Res.*, **26**(2-3), 77-98.

Lee, S.L., Ting, L.C. and Shanmugam, N.E. (1994), "Nonlinear analysis of I-beam to box column connections", *J. Constr. Steel Res.*, **28**(3), 257-278.

Mirghaderi, S.R., Shahabeddin, T. and Keshavarzi, F. (2010), "I-beam to box-column connection by a vertical plate passing through the column", *Eng. Struct.*, **32**(8), 2034-2048.

Miura, K. and Makino, Y. (2001), "Testing of beam-to-RHS column connections without weld access holes", *Proceedings of the 11th International Offshore and Polar Engineering Conference*, San Francisco, CA, USA, May, pp. 37-44.

Nie, J.G., Qin, K. and Cai, C.S. (2008a), "Seismic behavior of connections composed of CFSSTCs and steel-concrete composite beams-experimental study", *J. Constr. Steel Res*, **64**(10), 1178-1191.

Nie, J.G., Qin, K. and Cai, C.S. (2008b), "Seismic behavior of connections composed of CFSSTCs and steel-concrete composite beams-finite element analysis", *J. Constr. Steel Res*, **64**(6), 680-688.

Nie, J.G., Qin, K. and Cai, C.S. (2009), "Seismic behavior of composite connections-flexural capacity analysis", *J. Constr. Steel Res*, **65**(5), 1112-1120.

Nishiyama, I., Fujimoto, T., Fukumoto, T. and Yoshioka, K. (2004), "Inelastic force-deformation response of joint shear panels in beam-column moment connections to concrete-filled tubes", *J. Struct. Eng.*, **130**(2), 244-252.

Popov, E.P. (1987), "Panel zone flexibility in seismic moment joints", *J. Constr. Steel Res.*, **8**, 91-118.

Qin, Y., Chen, Z. and Wang, X. (2014a), "Elastoplastic behavior of through-diaphragm connections to concrete-filled rectangular tubular columns", *J. Constr. Steel Res.*, **93**, 88-96.

Qin, Y., Chen, Z., Wang, X. and Zhou, T. (2014b), "Seismic behavior of through-diaphragm connections between CFRT columns and steel beams-experimental study", *Adv. Steel Constr.*, **10**(3), 351-371.

Qiu, W., Jiang, M., Pan, S. and Zhang, Z. (2013), "Seismic responses of composite bridge piers with CFT columns embedded inside", *Steel Compos. Struct., Int. J.*, **15**(3), 343-355.

Rong, B., Chen, Z.H., Zhang, R.Y., Apostolos, F. and Yang, N. (2012), "Experimental and analytical investigation of the behavior of diaphragm-through joints of concrete-filled tubular columns", *J. Mech. Mater. Struct.*, **7**(10), 909-929.

Shahabeddin, T., Mirghaderi, S.R. and Keshavarzi, F. (2012), "Moment connection between I-beam and built-up square column by a diagonal through plate", *J. Constr. Steel Res.*, **70**, 385-401.

Shanmugam, N.E. and Ting, L.C. (1995), "Welded interior box-column to I-beam connections", *Eng. Struct.*, **121**(5), 824-830.

Wang, Q.T. and Chang, X. (2013), "Analysis of concrete-filled steel tubular columns with "T" shaped cross section (CFTTS)", *Steel Compos. Struct.*, *Int. J.*, **15**(1), 41-55.

Wang, W.D., Han, L.H. and Zhao, X.L. (2009), "Analytical behavior of Frames with steel beams to concrete-filled steel tubular column", *J. Constr. Steel Res.*, **65**(3), 497-508.

CC